Metadata of the chapter that will be visualized in SpringerLink

Book Title	Cavitation Instabilities and Rotordynamic Effects in Turbopumps and Hydroturbines
Series Title	
Chapter Title	Experimental Methods for the Study of Hydrodynamic Cavitation
Copyright Year	2017
Copyright HolderName	CISM International Centre for Mechanical Sciences

Corresponding Author	Family Name	**Ceccio**
	Particle	
	Given Name	**Steven L.**
	Prefix	
	Suffix	
	Division	Department of Naval Architecture and Marine Engineering
	Organization	University of Michigan
	Address	Ann Arbor, MI, USA
	Email	ceccio@umich.edu
Author	Family Name	**Mäkiharju**
	Particle	
	Given Name	**Simo A.**
	Prefix	
	Suffix	
	Division	Department of Mechanical Engineering
	Organization	University of California
	Address	CA, Berkeley, USA
	Email	

Abstract	A review of traditional and novel experimental methods for the investigation of hydrodynamic cavitation is presented. The importance of water quality is discussed, along with its characterization and management. Methods for the direct and indirect experimental determination of cavitation inception are presented. Along with traditional optical visualization, methods of measuring developed cavitation are described, including point and surface electrical probes, optical bubble probes, acoustic measurements, and indirect measurements of noise and vibration. Recent developments in the use of ionizing radiation as a means to visualize cavitating flows are also discussed.

Experimental Methods for the Study of Hydrodynamic Cavitation

Steven L. Ceccio and Simo A. Mäkiharju

Abstract A review of traditional and novel experimental methods for the investigation of hydrodynamic cavitation is presented. The importance of water quality is discussed, along with its characterization and management. Methods for the direct and indirect experimental determination of cavitation inception are presented. Along with traditional optical visualization, methods of measuring developed cavitation are described, including point and surface electrical probes, optical bubble probes, acoustic measurements, and indirect measurements of noise and vibration. Recent developments in the use of ionizing radiation as a means to visualize cavitating flows are also discussed.

1 Introduction

Hydrodynamic cavitation can occur in a variety of important liquid flows, including those associated with turbines, pumps, and other turbomachinery, ship propulsors, ventricular assist devices, fuel injectors, and other macro and micro fluidic systems. The presence of cavitation can degrade the performance of these devices, and can lead to excessive noise, vibration, and erosion. However, cavitation can be used to enhance the performance of some systems, such as high-speed underwater vehicles (Ceccio 2010).

Given the complexity of many cavitating flows, engineers have often resorted to experimental testing in order to reveal the presence of cavitation and its effect on system performance. And, for physically large systems such as turbines and propulsors, testing of scale models is often the only practical means of developing an optimized design before its manufacture at full scale. Experimental testing has also been used

S.L. Ceccio (✉)
Department of Naval Architecture and Marine Engineering, University of Michigan, Ann Arbor MI, USA
e-mail: ceccio@umich.edu

S.A. Mäkiharju
Department of Mechanical Engineering, University of California, CA, Berkeley, USA

L. d'Agostino and M.V. Salvetti (eds.), *Cavitation Instabilities and Rotordynamic Effects in Turbopumps and Hydroturbines*, CISM International Centre for Mechanical Sciences 575, DOI 10.1007/978-3-319-49719-8_2

to illuminate the basic processes of cavitating flows, usually through the examination of canonical flows that may be used to study specific cavitating flow processes, such as flows with variable area ducts and Venturis, and over headforms and hydrofoils.

The goal of this chapter is to review some experimental methods that have been successfully employed to study hydrodynamic cavitation (e.g., cavitation produced by flowing liquids). However, many of the methods are also useful for examination of cavitation produced by acoustic fields as well as other gas–liquid multiphase flows, including boiling flows. And some are also applicable to gas–solid and liquid–solid flows as well. The focus will be on the experimental methods that are available to researchers as they examine the flow processes that lead to cavitation inception, its development, and its effect on system performance, and its erosive potential rather than the test facility itself. But, a brief summary is provided here.

Experimental examination of hydrodynamic cavitation is often performed in a dedicated test facility. These can be broadly classified into flow loops and towing tanks. In the former, a prime mover delivers liquid (usually trough flow conditioners and a contraction) to the inlet of a test section where the cavitating flow will be examined. The flow is then returned (usually after passing through a diffuser where the pressure rises) to the prime mover to continue recirculation. Examples of modern cavitation tunnels are the Grand Tunnel Hydrodynamique (GTH) in France (Lecoffre et al. 1987), the Large Cavitation Channel (LCC) in the U.S.A. (Etter et al. 2005), and the Hydrodynamics and Cavitation Tunnel (HYKAT) in Germany (Wetzel and Arndt 1994a; Wetzel and Arndt 1994b). Turbomachinery may be tested with closed recirculating flow loops as well, as described by Avellan et al. (1987). Cavitation may also be studied by towing a test article in a stationary liquid, and facilities have been developed to allow for the ambient pressure over the free surface to be varied such that cavitation can form under a variety of flow conditions, such as the Depressurized Wave Basin in The Netherlands (Van der Kooij and De Bruijn 1984). The International Towing Tank Committee (ITTC) offers a catalog of many of these facilities, and Brandner et al. (2007) describe the recent design of a modern cavitation tunnel.

The capabilities and quality of the test facility is, of course, of central importance to the conduct of experimental investigations of cavitating flows. Many of the criteria used to assess a cavitation test facility are identical to those used for any aerodynamic or hydrodynamic test apparatus, including the uniformity and quality of the freestream flow, including the level of freestream turbulence, and the precision and range over which flow speed and pressure may be fixed. Many of the design requirements and approaches of subsonic wind tunnels presented by Rae and Pope (1984) apply equally to conventional water tunnels.

The acoustic characteristics of a cavitation flow facility may also be important to manage, as the acoustic emission of cavitation may be an important aspect of the testing program. The recently developed cavitation flow facility of the Japan Defense Agency is a modern example of a channel developed with these acoustic considerations (Sato et al. 2003). The tunnel was designed to reduce the amount of background noise and reverberation to improve the signal-to-noise ratio of for both noncavitating and cavitating flows. Finally, an important consideration for cavitating flow is management of the freestream water quality, which will be discussed below.

2 Characterization and Management of Water Quality

The inception and development of cavitation can be strongly related to the amount of free and dissolved gas within the cavitating liquid. Liquid that is supersaturated with dissolved gas and has many large free gas nuclei would be considered “weak”, and cavitation may form where the liquid pressure falls below vapor pressure. Conversely, liquid that is undersaturated with dissolved gas and has few free gas nuclei can sustain pressures below vapor pressure (e.g., can be in tension), and is considered “strong”. Determination and control of the liquids cavitation “water quality” or “susceptibility” is an important consideration for many experimental studies of cavitating flows. Discussions of the importance of water quality with regard to the conduct and interpretation of cavitation experiments are found in Lecoffre and Bonnin (1979), Kuiper (1985), Gindroz and Billet (1998), Arndt (2002), and Atlar (2002).

Cavitation inception occurs when a reduction in the liquid pressure results in a local pressure below the vapor pressure, and the liquid begins to change phase into vapor. Homogeneous nucleation process can occur in the bulk of the liquid as a result of inclusions that naturally form due to the random motion of the liquid molecules (Brennen 1995). Homogeneous nucleation typically requires a significant level of liquid tension, and ultraclean water can sustain tensions of over 30 MPa at room temperature (Mørch 2007). Yet, for many practical situations, cavitation incepts as a result of heterogeneous nucleation whereby nucleation sites within the bulk of the fluid or at solid boundaries grow when exposed to sufficiently strong tension. The characterization of the fluid’s susceptibility to nucleation is an important aspect of many cavitation studies, especially those concerned with inception. In turn, the susceptibility of the flow is related to both the free and dissolved gas content as well as the nature of potential surfaces and flow-borne nucleation sites.

Water quality can also affect developed cavitation. For example, the presence of many freestream nuclei can lead to the suppression of sheet cavitation through the formation of traveling bubbles upstream of the cavity separation location (Li and Ceccio 1996; Keller 2001), and diffusion of dissolved gas into a developed tip vortex can significantly alter its core size (Gowing et al. 1995). As a consequence, it is incumbent upon the cavitation research engineer to adequately characterize and, if possible, manage the facility’s water quality before conducting experimental studies and scale testing.

2.1 Dissolved Gas Content

Henry's law states that the equilibrium amount of a dissolved gas in a liquid at a given temperature is related to the partial pressure of the gas. When the gas concentration is at equilibrium, this is the saturated condition. Then, a reduction in the liquid pressure would result in supersaturation, and outgassing can occur. Likewise, if the pressure of the liquid is increased, the undersaturated liquid can dissolve more free gas. Hence, as a saturated liquid flows into regions of low pressure and cavitates, it is possible that significant amounts of outgassing may accompany any vaporization. Moreover, the level of gas saturation will influence the stability of free gas nuclei, which will be discussed below. The total dissolved gas content can be determined using a van Slyke apparatus developed for measurement of blood gas (Simoni et al. 2002). The van Slyke apparatus uses a vacuum placed over the liquid sample to produce outgassing, and it is quite accurate. Traditionally, the vacuum was created by the movement of a mercury manometer, which has led to its replacement by other methods that do not require the manual manipulation of mercury reservoirs.

For many practical applications, the cavitating liquid is water, and the dissolved gases are the main components of air, molecular nitrogen, and oxygen. But, other dissolved gases may be of interest, especially noble gases (Rooze et al. 2013). Measurement of dissolved gas content can be achieved with a Total Dissolved Gas Pressure (TDGP) probe. A sample of the liquid is placed in a probe beneath a headspace of gas at a known pressure that is separated from the liquid by a permeable membrane. Over a period the transfer of dissolved gas into or out of the headspace will change the gas pressure, and this change can then be related to the original dissolved gas concentration of the liquid sample. In order to relate the pressure change to the gas concentration, the chemical composition of the dissolved gases must be known, and some systems combine the probe with a separate instrument to sample and characterize the composition of the gas released into the headspace. For air dissolved in water, it is often assumed that the ratio of the dissolved gases track the ratio of nitrogen and oxygen in air at standard conditions (Yu and Ceccio 1997; Lee et al. 2016). In fact, in many test facilities, only the dissolved oxygen is measured, and it is assumed that the level of oxygen saturation parallels the overall dissolved air concentration. Dissolved oxygen (DO) probes employ a measurement technique similar to that of pH meters. Two electrodes are suspended in a liquid electrolyte, which is separated from the test sample by a semipermeable membrane. A low DC voltage is applied between the electrodes within the electrolyte, and when oxygen molecules from the test liquid cross the membrane, the magnitude of current between the electrodes will change.

337316_1_En_2_Chapter ☑ TYPESET ☐ DISK ☐ LE ☑ CP Disp.:3/12/2016 Pages: 31 Layout: T1-Standard

2.2 Free Gas Content and Cavitation Nuclei

Measurement of the free gas content is more difficult. The intent is to characterize the nucleation sites in the freestream liquid, and a variety of methods have been proposed and evaluated (Lecoffre and Bonnin 1979; Oldenziel 1982; d'Agostino and Acosta 1991; Ceccio et al. 1995; Billet 1985; Pham et al. 1999). Freestream nuclei are any inclusion in the fluid that will cavitate when exposed to a sufficient tension (as opposed to surface nucleation sites which reside on flow boundaries). An ideal nucleus is a clean gas bubble, and the nucleation characteristics of such a bubble can be readily predicted. However, a wider variety of nucleation sites exist in the flow, including gas pockets on the surface of particles and bubbles that have significant surface contamination. Nevertheless, ~~is~~ useful to review the basic nucleation process of a clean bubble in order to give us a reference to compare with practically observed nuclei.

Consider a nucleus that is a clean gas bubble with a radius R_N that contains vapor and noncondensable gas. The pressure inside the bubble, $P_B = P_V + P_G$ is the sum of the partial pressures of the vapor and noncondensable gas, respectively. This pressure is balanced by the liquid pressure on the bubble surface, P_∞, such that

$$P_\infty = P_V + P_G - \frac{2S}{R_N},$$

where S is the surface tension. When a nucleus experiences a drop in the surrounding liquid pressure, the radius may grow quasi-statically from its initial equilibrium radius to a larger equilibrium radius. However, if a tension is applied below a critical value, $P_V = P_C - P_\infty$, the radius will grow unboundedly. This critical tension is given by

$$\frac{4S}{3R_N} < P_V - P_\infty < \frac{2S}{R_N}$$

(Brennen 1995). Note that since the fluid is in tension, $P_V > P_\infty$, and that the static pressure is in fact negative. While not all nuclei are clean bubbles, the fluids nuclei content is often reported as a distribution of nuclei with a given critical radius, R_C. This is the radius that corresponds to the required critical pressure, P_C, needed to produce explosive growth of the nucleus. Therefore, the nuclei content of a liquid is typically reported as a Nuclei Number Density Distribution (*NNDD*) as a function of R_C, where $NNDD(R_C)$ has units of [Number]/[Length]$^{-4}$. Then, the number of nuclei over a range of critical radius ΔR_C is given by $NNDD(R_C) \cdot R_C$. Alternatively, if the bin size of the distribution is fixed, the Nuclei Number Distribution (*NND*) with units of [Number]/[Length]$^{-3}$ can be presented, as shown in Fig. 1 (Chang et al. 2011). The typical range of nuclei critical radii in test facilities spans 1 micron < R_C < 500 micron, and the critical tensions range from $0 > P_C > -100$ kPa. Nuclei concentrations can range widely, with order 1 per cubic centimeter for the smallest nuclei and order 10 per cubic meter for the largest (Gindroz 1998).

Fig. 1 Example nuclei concentration measured with a centerbody Venturi (Chang and Ceccio 2011). The different spectra are for varying freestream dissolved oxygen levels and concentrations of long-chain polymer

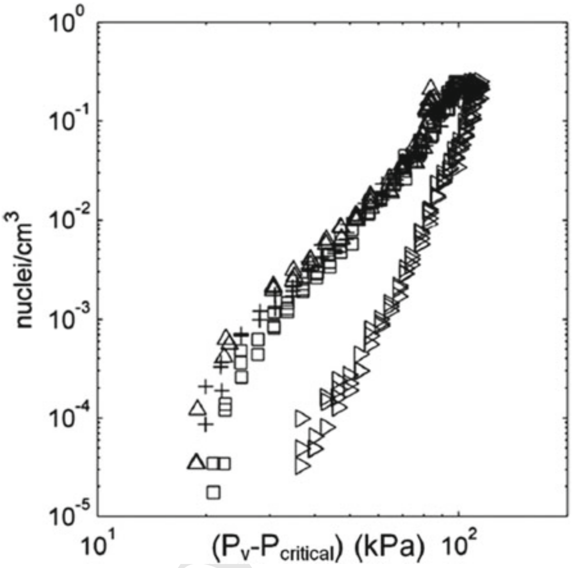

2.3 *Direct Measurement of the Cavitation Nuclei Distribution*

Measurement of the nuclei distribution can be accomplished with both direct and inferred means. In direct methods, a sample of the flow is exposed to a known tension, resulting in the cavitation of nuclei that incepts at (or above) that critical pressure. These devices are collectively known as Cavitation Susceptibility Meters (CSMs), as first discussed by Schiebe (1972). The most common CSM consists of a simple venture through which the liquid is passed. The pressure in the throat is measured or inferred, the occurrence of single cavitation events are detected optically, electrically, and/or acoustically. CSMs of this type have been developed by Oldenziel (1982), Chahine and Shen (1986), d'Agostino and Acosta (1991), Chambers et al. (2000), for example. During typical operation, a sample of the freestream liquid is drawn from the flow facility and delivered to the CSM inlet. Care must be taken to insure that the sampling process does not significantly alter the nuclei distribution itself. Then, the flow is passed through the CSM. Changing the flow rate then varies the throat pressure, and the number of cavitation inception events is counted at each level of throat tension. Knowledge of the flow rate and throat tension yields the concentration of nuclei that incept at or above the given tension. This data is then converted into the nuclei number distribution.

One limitation of Venturi-based CSMs is the limited volume of the throat. If the nuclei distribution is too dense, multiple bubbles may simultaneously form in the throat, creating a blockage. A solution is to use a centerbody Venturi (Lavigne 1991), as shown in Fig. 2. Now the high-tension region is an annulus of fluid around the centerbody, increasing the volume of liquid that is in tension. Keller (1987) developed

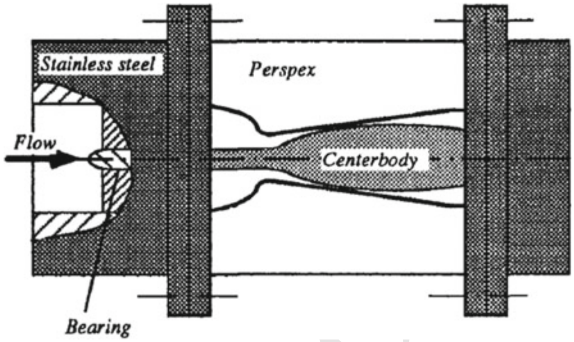

Fig. 2 Schematic diagram of a centerbody venturi cavitation susceptibility meter (Gindroz and Billet 1998)

a CSM that used a swirling flow passed through a vortex to create the region of low pressure.

While the operation of a CSM can be somewhat cumbersome, it is a device that directly measures the number of cavitation nuclei and their critical tension. It is important to note that not all nuclei are clean gas bubbles. In fact, particulates with small gas pockets on their surface can readily act as nuclei, and free gas bubbles can be coated by an organic skin, effectively modifying their interfacial properties. (Mørch 2007). Hence, a measurement of the size of the nucleus in the flow may not necessarily yield an accurate measure of its critical tension.

2.4 Indirect Measurement of the Cavitation Nuclei Distribution

Indirect measurement of the nuclei distribution can be operationally advantageous, especially if online or in situ measurement is required. Unlike CSMs, indirect measurements ascertain some aspect of suspected nuclei, such as its light or acoustic scattering properties. From this, the critical tension of the detected nucleus is inferred. As noted above, this relationship may not be easily determined. Nevertheless, the advantages of indirect methods have motived their development and use.

Bubble populations in liquids can be determined via acoustic scattering. Duraiswami et al. (1998) and Chahine and Kalumuck (2003) report on a method that employs the dispersion of sound passing through a bubbly medium. Both the attenuation and phase velocity are measured, and analytical relationships are used to invert these data into the bubble population. Once the bubble population is determined, the cavitation susceptibility can be inferred.

Light scattering can be used to detect the presence of nuclei in the flow (Keller 1972). Mie scattering by small spherical nuclei can be detected as they pass through a focused region of laser light, for example. A somewhat more sophisticated method employs Phase Doppler Anemometry (PDA), where multiple detectors are used to record the light scattered from a particle passing through the probe volume made by two crossed laser beams (Tanger and Weitendorf 1992). PDA systems can more readily determine the radius and velocity of the presumably spherical nucleus passing through the control volume. Care must be taken to relate the measured event rate to the actual nuclei density, since the effective measurement volume may not be easily determined given that nuclei may not pass directly through the measurement volume, for example. And, it is important to discriminate between bubbles and particles as they pass through the probe volume.

A direct optical measurement of the nuclei distribution can be made using holography (Katz et al. 1984; Katz and Sheng 2010). Holographic imaging can yield the absolute nuclei distribution in a volume of fluid, and with proper resolution, can be used to distinguish between bubbles, particulates, and other contaminants. Hence, holography is often used as the calibration standard for other nuclei measurement systems. Holographic systems have been used to measure nuclei distributions both in the laboratory and in the environment (Katz and Acosta 1981; O'Hern et al. 1985). Kawanami et al. (2002) used laser holography to study the structure of a cloud shed from a hydrofoil and estimated the bubble size distribution. Holography is not typically used as a routine nuclei measurement method, but recent advances in both camera technology and digital processing have made its everyday use more feasible.

2.5 Management of Water Quality

Characterization of the freestream dissolved and free gas content can be an essential component of any experimental test and evaluation effort. Moreover, it may be advantageous to actively manage these quantities through the addition or removal of dissolved gas and freestream nuclei. Besides filtering, the most basic method to control the water quality is through degassing the bulk of the test liquid, and deaeration is a common practice to reduce both the free and dissolved gas during testing. Typically, the dissolved gas concentration will be reduced to levels below 50.

Control of the water quality can be improved via the active management of the free and dissolved gas content. The major flow facilities that have implemented these systems include the Grand Tunnel Hydrodynamique in France (Lecoffre et al. 1987) and the Australian Maritime College Cavitation Tunnel (Brandner et al. 2007). Figure 3 shows an image of latter facility that highlights the means of gas control. The facility is equipped with bulk degassing systems to control the average dissolved gas concentration. Additionally, small gas bubbles can be controllably injected directly into the flow upstream of the test section, while both small and large gas bubbles are removed downstream of the test section via gravity separation, coalescence, and resorption. In this way, the nuclei distribution can be prescribed and maintained during an experiment.

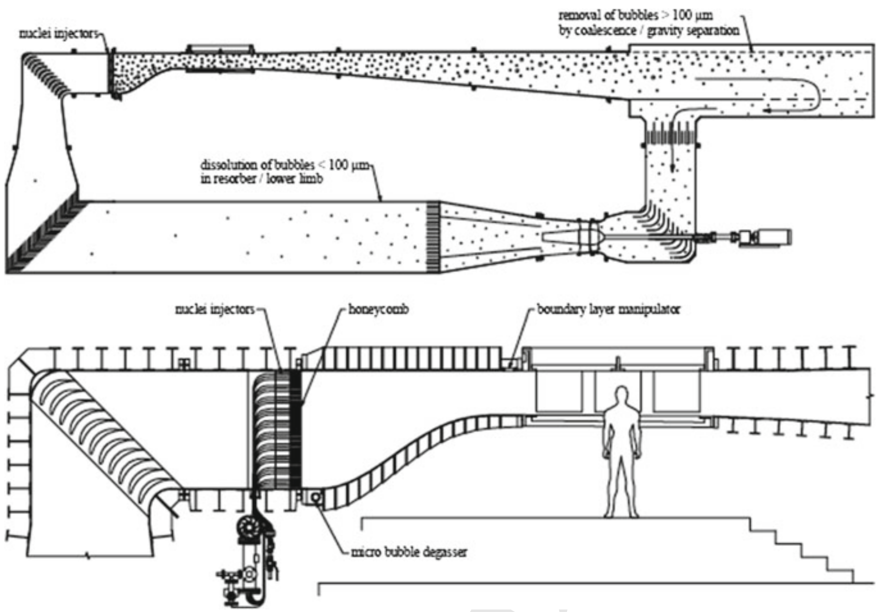

Fig. 3 A schematic diagram of the water quality management systems of the Australian Maritime College Cavitation Tunnel (Brandner et al. 2007). Nuclei can be injected upstream of the test section, and the tunnel is designed to remove gas by separation, coalescence, and resorption

3 Detection and Measurement of Incipient Cavitation

Cavitation inception occurs when cavitation is first observed in the flow, and the determination of inception conditions is important characterization of the flow itself as well as an important consideration for the scaling of the performance of model hydraulic systems. Inception usually occurs when the first freestream or surface nuclei encounter sufficient tension in the flow field to cavitate. Since a distribution of nuclei exists in the flow, and the pressure field producing the tension can often have important contributions from flow unsteadiness, inception is usually a stochastic process. Therefore, the average flow conditions under which inception is determined is, many cases, subjective. Moreover, the extent of cavitation chosen as necessary to call inception can vary widely. In some cases, such as the characterization of naval systems, only a minimal amount of cavitation is required to call inception, and the cavitation may not be easily visible to the naked eye. Conversely, limited cavitation may not be of practical interest to the operators of industrial hydraulic systems, and inception would be called only when the amount of cavitation begins to alter the performance of the device. And finally, proper use of inception observations in the scaling of model hydraulic systems to full scale is also of vital importance. Acosta and Parkin (1975) and Rood (1991) review the basic elements of cavitation inception for a variety of cavitation forms.

3.1 *Detection of Inception with Acoustic, Vibration, and Force Measurements*

Since the presence of incipient cavitation will many times be accompanied by emission of sound from the cavitating nuclei, the detection of inception is often accomplished through acoustic means. Hydrophones can be placed directly within the flow field (Ran and Katz 1994), within the cavitating test article itself (Ceccio and Brennen 1991; Kuhn de Chizelle et al. 1995) or in acoustically coupled chambers that are separated from the flow by an acoustic window (Choi and Ceccio 2007). Since the acoustic impedance of acrylic (3.1×10^6 Pa s / m^3) is only about twice that of

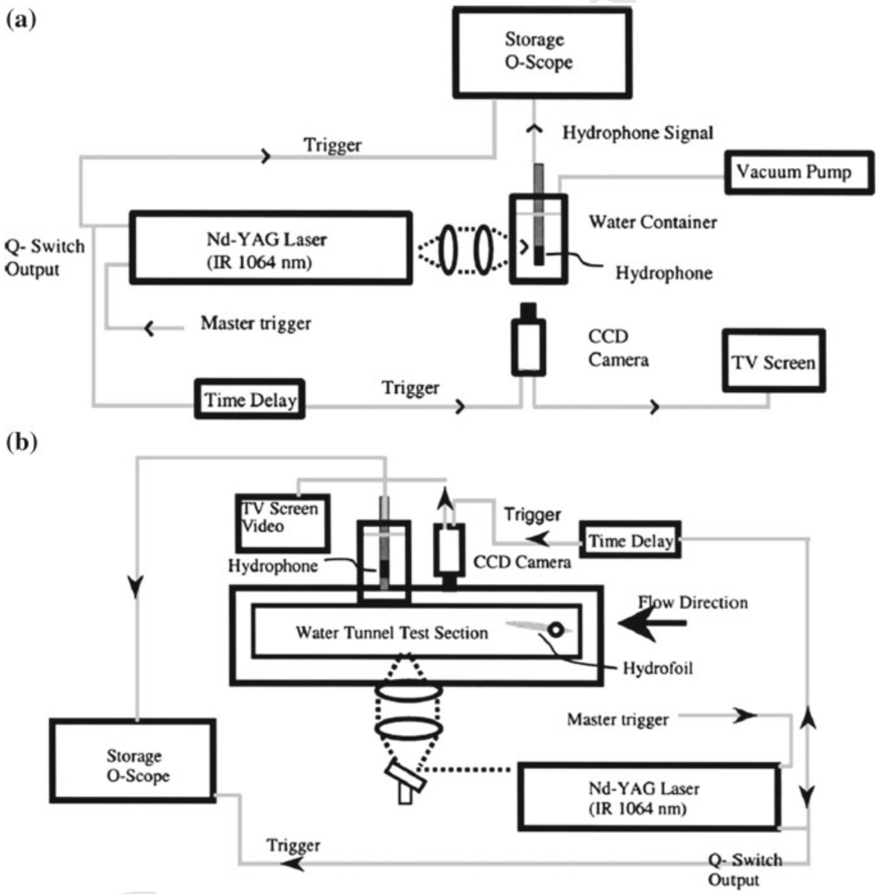

Fig. 4 Schematic diagram of the quiescent laser-induced cavitation bubble experiment (**a**) and a bubble–vortex interaction experiment (**b**). A single laser pulse is used to create a cavitation bubble in the bulk of the fluid from Oweis et al. (2004). The acoustic emission of the bubble is captured with a hydrophone within the flow (**a**) and in an external chamber through an acoustic window (**b**)

337316_1_En_2_Chapter ☑ TYPESET ☐ DISK ☐ LE ☑ CP Disp.:3/12/2016 Pages: 31 Layout: T1-Standard

water (1.5×10^6 Pa s / m^3), it is commonly used as a rigid acoustic flow boundary. (A metal boundary would be much more reflective, with impedance mismatches in excess of ten times that of water.) Fig. 4 shows two typical setups from Oweis et al. (2004). AQ1

The noise produced by incipient cavitation bubbles often takes to form of discrete bursts or pulses, and example sound traces are shown in Fig. 5 from Chang and Ceccio (2011). In this case, the bubbles were formed in the cores of stretched vortices,

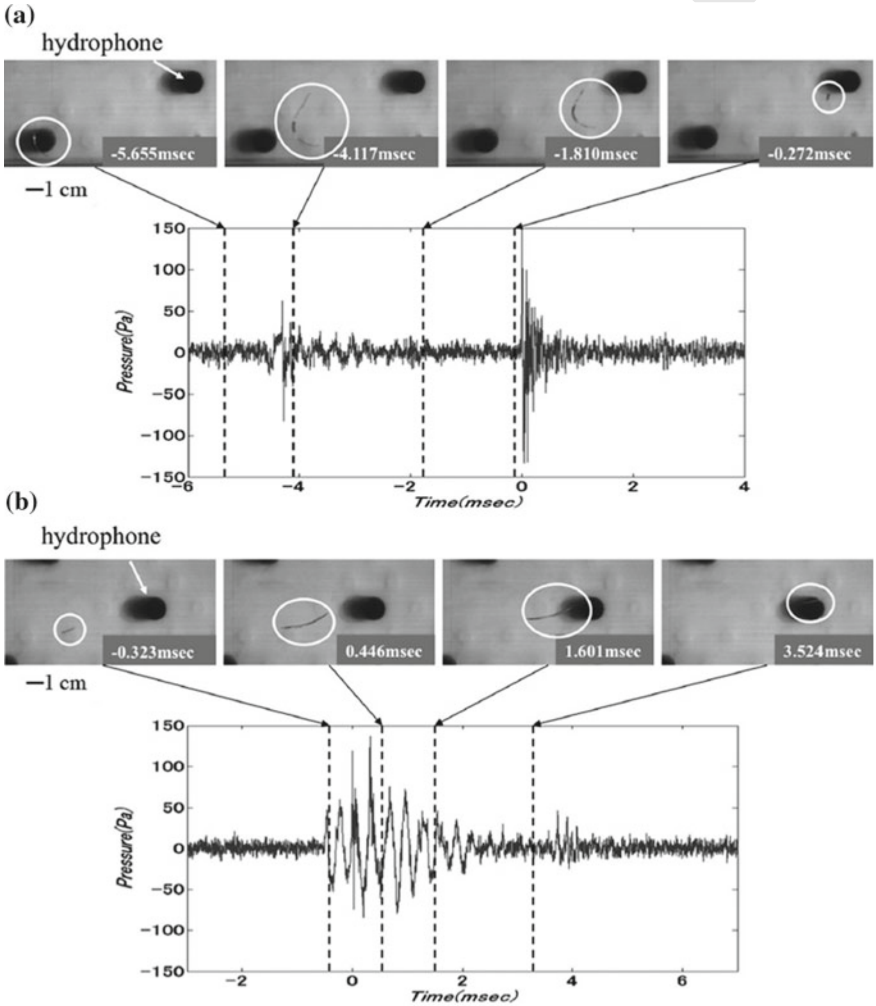

Fig. 5 Images and sound traces of a growing and collapsing vortex cavitation bubble in the secondary vortex producing an **a** acoustic "pop" and **b** a "chirp". The broadband acoustic pulse was abrupt lasting approximately 1 ms (Chang and Ceccio 2011)

and the sounds recorded from individual bubbles could be a pulse ("pop") or a periodic tonal burst ("chirp"). The hydrophone array can be seen in the image, and, in this case, an array of hydrophones was used to localize the sound source (Chang and Dowling 2009).

As the cavitation develops, the amount of sound emitted and the cavitation's effect on the overall flow begins to increase. Hence, measurement of vibration and changes to the system performance (e.g., lift coefficient, flow coefficient, efficiency) can be used to call inception. See, for example, Arndt (1981), McNulty and Pearsall (1982), Shen and Dimotakis (1989), and Koivula (2000). Indirect methods of inception detection are often calibrated against visual observations when optical access to the incepting flow is available. Escaler et al. (2006) report on a comprehensive study that illustrates how cavitation inception can be detected using measurements of structural vibrations, acoustic emissions, and hydrodynamic pressures measured in turbomachinery where optical access may be limited or unavailable.

3.2 Optical Measurement and Light Scattering for Inception Detection

Direct visual observations of incepting nuclei are often used to call inception. Traditionally, the flow is illuminated with stroboscopic lighting, and a human observer is tasked with determining which conditions have produced detectable and sustained cavitation. The availability of high-speed video systems have enabled the digital recording and analysis of the incepting flow, making inception calls with the naked human eye less common. However, at the first moments of inception, the cavitation bubbles may be quite small and difficult to locate; and they may occur infrequently. Such limited event rate cavitation inception is difficult to discern with visual detection alone, and the camera systems can be synchronized with acoustic detection systems (see, for example, Gopalan et al. (1999) and Chang and Ceccio (2011)). If the location of inception is known a priori, then focused light scattering can be used to detect the onset and rate of bubble formation. Keller (1972) developed such a system by directing a focused light source into the inception region of a headform and then into a photodetector. The presence of the bubble in the measurement volume would block the light to produce a signal.

4 Optical Measurement of the Cavitating Flow Field

Many optically based methods that have been developed for fluid measurements can also be effectively employed to study cavitating flows. General reviews of optical methods are provided by Goldstein (1996) and Tropea et al. (2007), and these methods and their applications are wide raging and varied. With this in mind, this section will concentrate on the use of optical methods in cavitating flows.

4.1 High-Speed Imaging

The need to study the dynamics of cavitation has stimulated the development of high-speed imaging. From the early work of Benjamin and Ellis (1966), Kling and Hammitt (1972), and Lauterborn and Bolle (1975), high-speed photography has played a key role in understanding bubbly dynamics and cavitation. A recent review by Thoroddsen et al. (2008) provides a good summary of the history and recent methods. As the resolution and frame rate of high-speed digital imaging systems has improved, the ability for detailed examination of cavitating flows has significantly improved. Frame rates of order 1 Khz with spatial resolution of $10^3 \times 10^3$ pixels are now commonly available, and cameras with much higher imaging speeds are commercially available. Ultrahigh-speed imaging systems have been created as well, with frame rates in excess of 1 million per second. Such systems can resolve the fine details of cavitation bubble dynamics, as shown by Lauterborn and Hentschel (1985), Ohl et al. (1995), and Obreschkow et al. (2006).

The study of high-speed bubble dynamics often requires the controlled creation of single or multiple bubbles. In many cases cited above, a laser pulse is focused to create the bubble in the imaging region of the camera. The bubble creation can then be synchronized with the imaging system. This technique can be used to controllably place nuclei into the freestream flow as well, as shown by Choi and Ceccio (2007). Figure 6 presents a time series from high-speed imaging of a laser-induced bubble from Ohl et al. (1998), including a schematic of the setup and an example of an aspherically collapsing bubble with detected luminescence. And, Fig. 7 shows images of a vortex cavitation bubble formed after a laser-induced nucleus was created within the upstream core of the vortex.

4.2 Laser Doppler Velocimetry and Light Scattering Methods

Laser Doppler Velocimetry (LDV) (also known as Laser Doppler Anemometry) is a well-established technique to measure local flow velocity. In this method, two beams of laser light are crossed within the flow domain to create a probe volume consisting of an interference pattern of light. As flow-borne particles pass through the probe volume, the scattered light from the fringe pattern is detected. The frequency of the light “burst” is related to the fringe spacing (and fringe velocity if one laser beam is frequency shifted) and the velocity of the particle. If it can be assumed that the particle travels at the local flow speed, inference of the particle velocity yields a nonintrusive measurement of the flow velocity. Laser beams with multiple colors (wavelengths) can be used to measure two or three components of the flow speed in the same probe volume. A comprehensive review of this method can be found in Durst (1982) and Goldstein (1996).

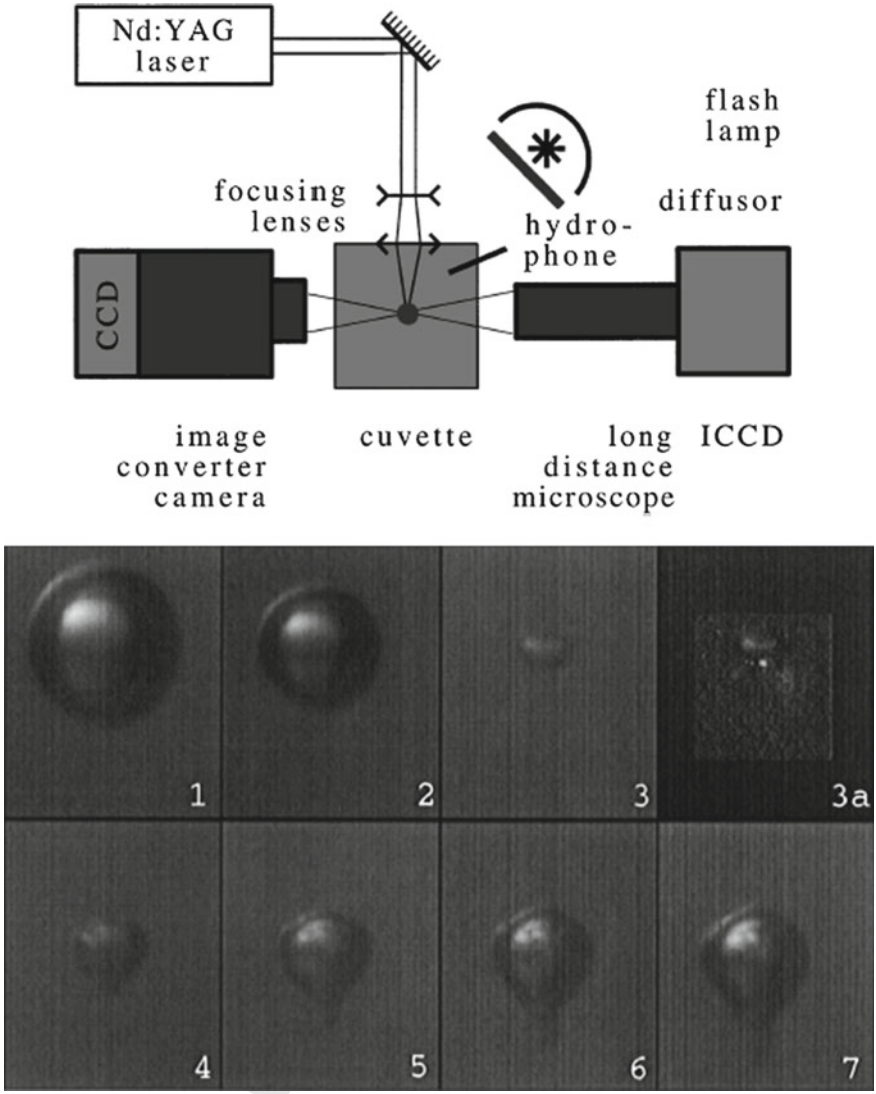

Fig. 6 High-speed imaging of a laser-induced bubble from Ohl et al. (1998). A schematic of the setup used to create the laser-induced bubbles is shown in along with images of an aspherically collapsing bubble with detected luminescence

LDV can be a useful method to examine cavitating flows. Kubota et al. (1989) used conditional sampling of the LDV for velocity measurements in a flow around a shedding partial cavity, as shown in Fig. 8. More recently, Roth et al. (2002) used similar methods to examine the cavitating flow in a fuel injector. In these cases, LDA was used to measure the velocity of the liquid flow around and outside the

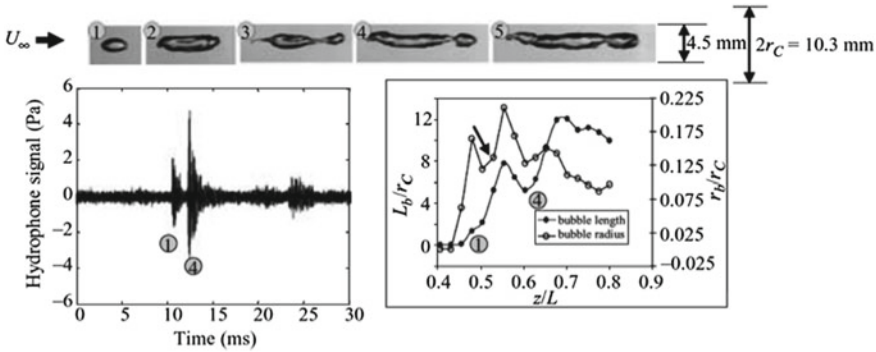

Fig. 7 Images of a vortex cavitation bubble created by a laser-induced nucleus; the images were used to compute the length and average radius of the bubble as a function of position within the Venturi. Also shown is the corresponding acoustic signal detected from a hydrophone Choi and Ceccio (2007)

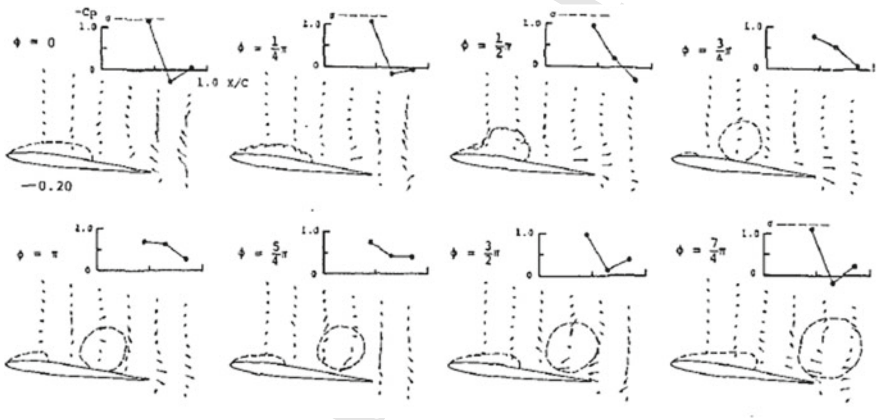

Fig. 8 Local measurements of flow velocity acquired with Laser Doppler Velocimetry were conditionally sampled and correlated to the measured surface pressure during the shedding of cloud cavitation on a hydrofoil (Kubota et al. 1989)

377 region developed cavitation. When employing LDV in this way, it is important to
378 determine if the flow tracers are small seed particles or small bubbles generated by
379 the cavitation itself since large bubbles may not necessarily behave as Lagrangian
380 flow tracers, especially in regions of high turbulence and shear.

337316_1_En_2_Chapter ☑ TYPESET ☐ DISK ☐ LE ☑ CP Disp.:3/12/2016 Pages: 31 Layout: T1-Standard

4.3 Particle Imaging Velocimetry

Particle Imaging Velocimetry (PIV) is a full-field method used to measure two or three components of the flow velocity in a plane or volume. In this method, the flow is densely seeded with flow tracers, and a plane or volume of the flow is illuminated with pulsed laser light. Two or more images of the flow tracers are compared to determine the motion of the tracers over a known time interval, and the motion of many particles are analyzed to determine the spatial distribution of velocities within the illuminated flow region. Since PIV's development in the 1990s there have been significant advances in its development and use, and a general review is provided by Adrian and Westerweel (2011). The use of PIV to study disperse multiphase flows has also been progressing. In these cases, care is taken to distinguish the tracer particles (which are intended to be nonintrusive) from those that constitute the disperse phase itself, such as larger particles or bubbles. Hassan et al. (1992), Lindken and Merzkirch (2002), and Balachandar and Eaton (2010) provided examples of PIV applied to such disperse multiphase flows.

As in the case of LDV, PIV can be used to study the low void fraction flow around developed cavitation. Examples include the work of Vogel and Lauterborn (1988), Leger and Ceccio (1998), Leger et al. (1998), Gopalan and Katz (2000), Laberteaux and Ceccio (2001a), Laberteaux and Ceccio (2001b), Dular et al. (2005), and Foeth et al. (2006). Figure 9 presents results from Foeth et al. (2006), who examined the dynamic flow around shedding partial cavities. The figure shows the steps needed to separate the images of the PIV tracer particles from the cavity and resulting bubbly flow. Synchronization of the image acquisition with periodically shedding cavity flows can yield phase-averaged flow data.

For limited cavitation, PIV can be used to interrogate the flow in and around the cavitation bubbles. Examples include Ran and Katz (1994), Iyer and Ceccio (2002), and Straka et al. (2010) who examined inception and bubble–vortex interactions in shear flows, and Wosnik et al. (2003) who examined the bubbly wake of supercavities. Figure 10 presents an example of the use of PIV in limited cavitating flows from Iyer and Ceccio (2002) who examined the influence of cavitation on the dynamics of a planar shear layer. The setup and an example image of the cavitating shear layer are shown in (a), and the mean flow and vorticity profiles are shown in (b) for increasing levels of cavitation (void fraction) in the shear layer. Recent advances in PIV systems include digital holographic PIV, micro-PIV, tomographic (volume) PIV, and high frame-rate cinemagraphic PIV. All of these methods have the potential to bring new insights into our understanding of cavitating flows.

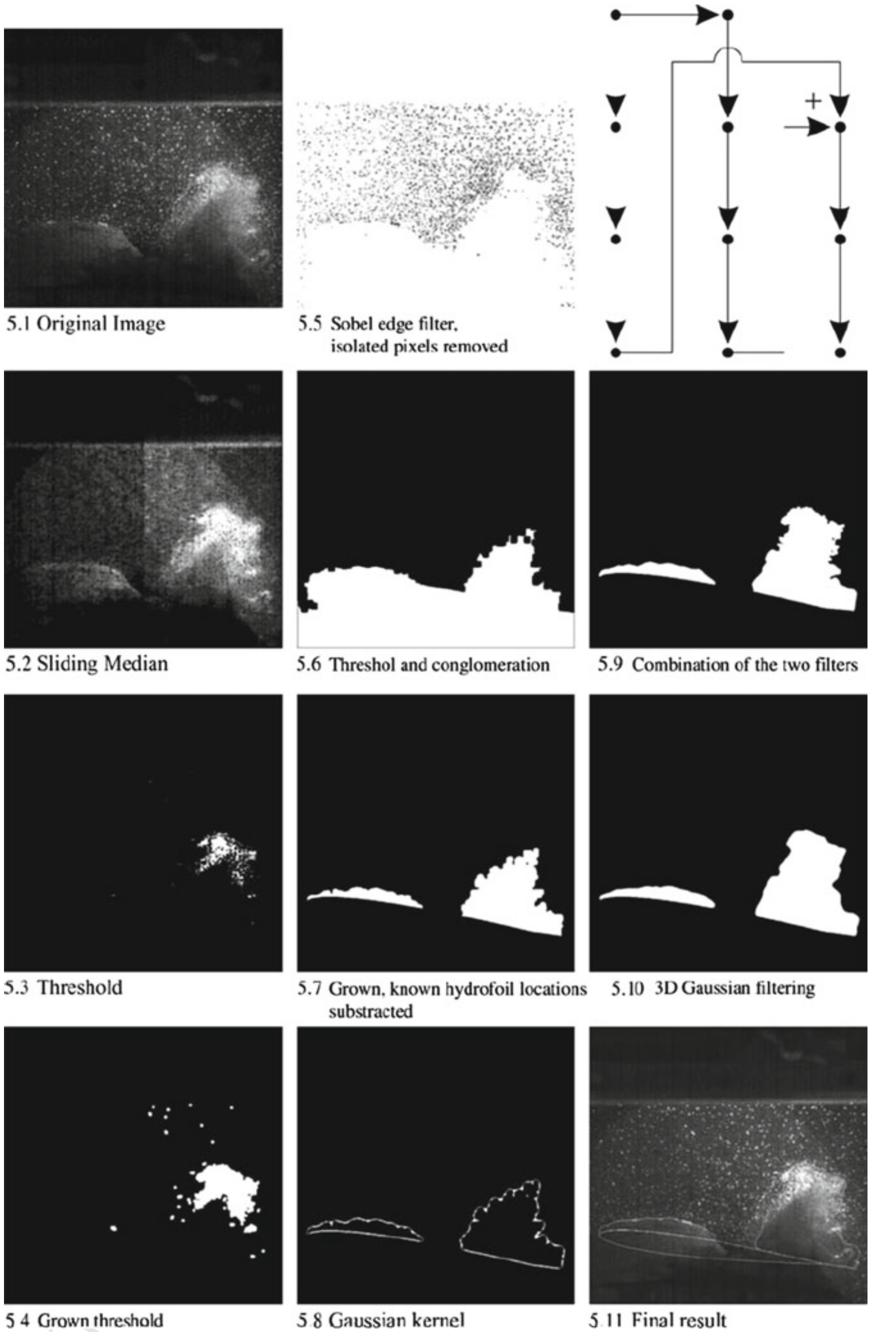

Fig. 9 The image processing steps employed by Foeth et al. (2006) to determine the flow field around a developed cavitation forming on a twisted hydrofoil

337316_1_En_2_Chapter ☑ TYPESET ☐ DISK ☐ LE ☑ CP Disp.:3/12/2016 Pages: 31 Layout: T1-Standard

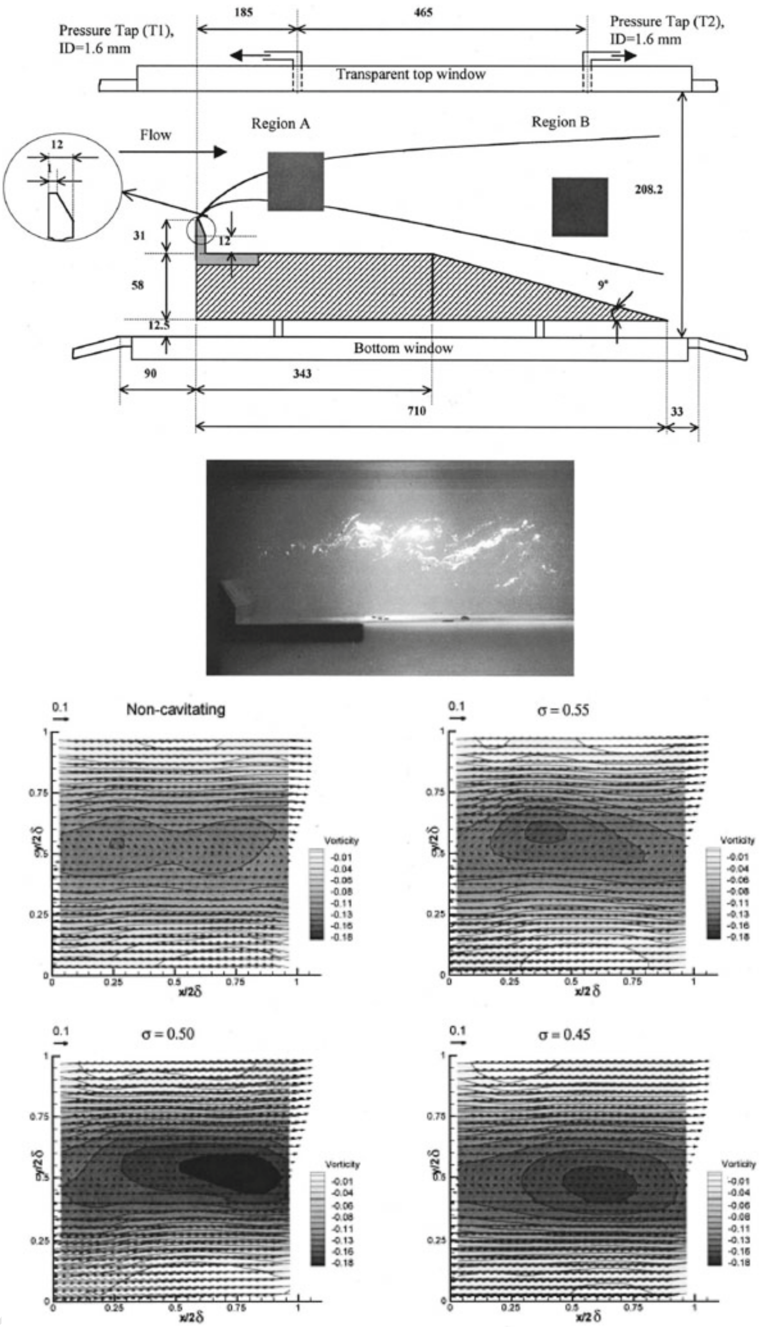

Fig. 10 Examination of the influence of cavitation on a shear layer using PIV (Iyer and Ceccio 2002). The setup and an example image of the cavitating shear layer are shown in (**a**) and (**b**), and the mean flow and vorticity profiles are shown in (c) for increasing levels of cavitation (void fraction) in the shear layer

5 Measurement of Cavity Flows with High Void Fraction

As the void fraction of the cavitating flow begins to exceed a few percent, the bubbly flow becomes opaque, and optical methods such as LDV and PIV begin to fail due to multiple scattering of the incident and reflected light. For very high void fraction flows, alternative techniques must be used, as described below.

5.1 Surface Pressure, Acceleration, and Forces

Cavitating flows with high void fraction often occur near solid boundaries, and it is therefore possible to place instruments close to or flush against the cavitating surface. The most common flush-mounted instruments measure the static and dynamic pressure. These measurements can be combined with local or average acceleration and forces on the test article to help elucidate the underlying flow. For example, Kjeldsen et al. (2000) measured the static and dynamic pressures on the surface of a cavitating hydrofoil, along with the time-varying lift force. Callenaere et al. (2001) employed dynamic and ultrasonic transducers to measure the reentrant flow beneath a partial cavity, and Le et al. (1993) employed arrays of dynamic pressure transducers to examine the unsteady pressures developed by partial cavitation. Escaler et al. (2006) illustrated how a range of nonoptical methods can be used to detect and quantity cavitation in turbomachinery, including external vibrations and noise signatures.

5.2 Electrical Impedance Probes

Since the gas and liquid phases of the cavitating flow have quite different electrical properties, measurements of the local or average mixture impedance can be used to infer the void fraction of the flow, and a review of these general methods is provided by Ceccio and George (1996). Measurement of the mixture impedance can be accomplished with flush-mounted electrodes or intrusive probes, albeit the latter may excessively perturb the cavitating flow. The electrodes can be made large enough to measure the bulk-averages void fraction, or small enough to measure the local void fraction or the passage of individual gas pockets. A high-frequency alternating current can be applied as the probing signal, making the temporal response of the transducers very rapid. However, as the path lines of the applied current are strongly affected by the presence of the gas phase, it is not always possible to fix the measurement volume of the probe. And, the relationship between the measure bulk impedance and the void fraction may not be straightforward. For bubbly flows, a mixture relationship can be developed that can relate the bulk impedance to the void fraction and electrical properties of the liquid and gas components (Hewitt 1978;

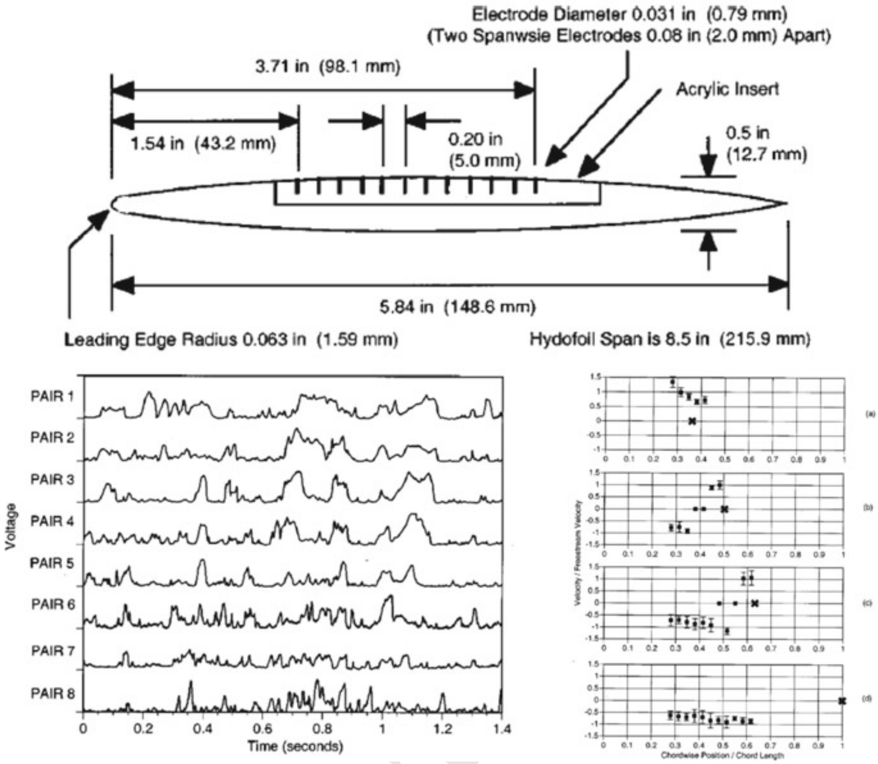

Fig. 11 The near-surface gas-phase velocity beneath a partial cavity measured with flush-mounted electrical impedance probes (George et al 2000a). The electrode locations on the hydrofoil (**a**), sample voltage signal transduced from the probes (**b**), and the gas-phase velocity determined through cross-correlation of the signals (**c**)

George et al. 2000b). But such relationships will generally fail for highly stratified flows.

Flush-mounted impedance probes have been used successfully to quantify cavitating flows. Examples include the work of Ceccio and Brennen (1991) and Kuhn de Chizelle et al. (1995) for the study of traveling bubble cavitation; and Ceccio and Brennen (1992), Pham et al. (1999), and George et al (2000a) for the study of partial cavitation. Cross-correlation of signals from multiple electrodes can be used to determine the gas-phase interface velocity, as reported by George et al (2000a) (Fig. 11). Intrusive conductivity probes with one or more electrode pairs have also been developed for gas–liquid flows, as discussed by Wu and Ishii (1999), Lucas and Mishra (2005), and Elbing et al. (2013).

5.3 Fiber Optic Probes

Fiber optic probes can be used to detect the presence of bubbles and gas–liquid interfaces via the difference in the index of refraction between the liquid and gas. The end of the fiber is placed in the flow, and light is directed toward the sharpened tip. If the tip is immersed in the pure liquid, the majority of the light will be transmitted into the fluid. But, if gas is present at the tip, the light will internally reflect within the fiber and return to its source to be detected. Fiber optic probes have been successfully employed to measure bubble size populations, average void fraction, phase speed, and interfacial area density, and a review is provided by Boyer et al. (2002) and Chang et al. (2003). The performance of optical and conductivity probes for measurement of bubbly flow was compared by Le Corre et al. (2003). The use of intrusive optical probes in cavitating flow has been limited due to the probes delicate construction and their ability to perturb the flow, but such probes were successfully used to study the dynamics of partial cavitation by Stutz and Reboud (2000) and Stutz (2003). Figure 12 presents the probe employed by Stutz and Reboud (2000) to measure the bubbly flow within a partial cavity, the time traces from two probes that can be used to measure the local volume fraction and phase speed, and an example data set showing the average volume fraction within the cavity. As in the case of electrical impedance probes, care must be taken to carefully determine how the signal transduced from the probe relates to the flow quantity of interest (e.g., bubble size and velocity) and what the influence volume of the probe may be. Single point probes have shown the best results when they are oriented in a flow with a strong rectilinear velocity and when the probe tip is small compared to the bubbles to be measured (Cartellier 1992; Mäkiharju et al. 2013).

Images of a high void fraction bubbly cavitating flow were acquired by Coutier-Delgosha et al. (2006) by traversing an endoscope within a partial cavity flow. They were able to demonstrate that the bubbly flow within the cavity often consists of highly distorted gas bubbled, as shown in Fig. 13. AQ2

5.4 Ionizing Radiation

The use of X-ray and gamma-ray densitometry and tomography for the study of multiphase flows has been well established, and reviews are provided by Kumar et al. (1997), George et al. (2000b), and Heindel (2011). These methods have also been applied for the study of high void fraction cavitating flows.

The underlying principal of these systems relies the material and density dependent attenuation coefficient of high-energy photons as they pass through the multiphase mixture. When a beam of high-energy X-ray photons, for example, encounters the mixture, a fraction of the photons passes through without scattering or absorption, and this fraction depends on the mixture's attenuation coefficient, μ, density, ρ, and thickness, x. For a beam encountering a domain with N distinct materials, the

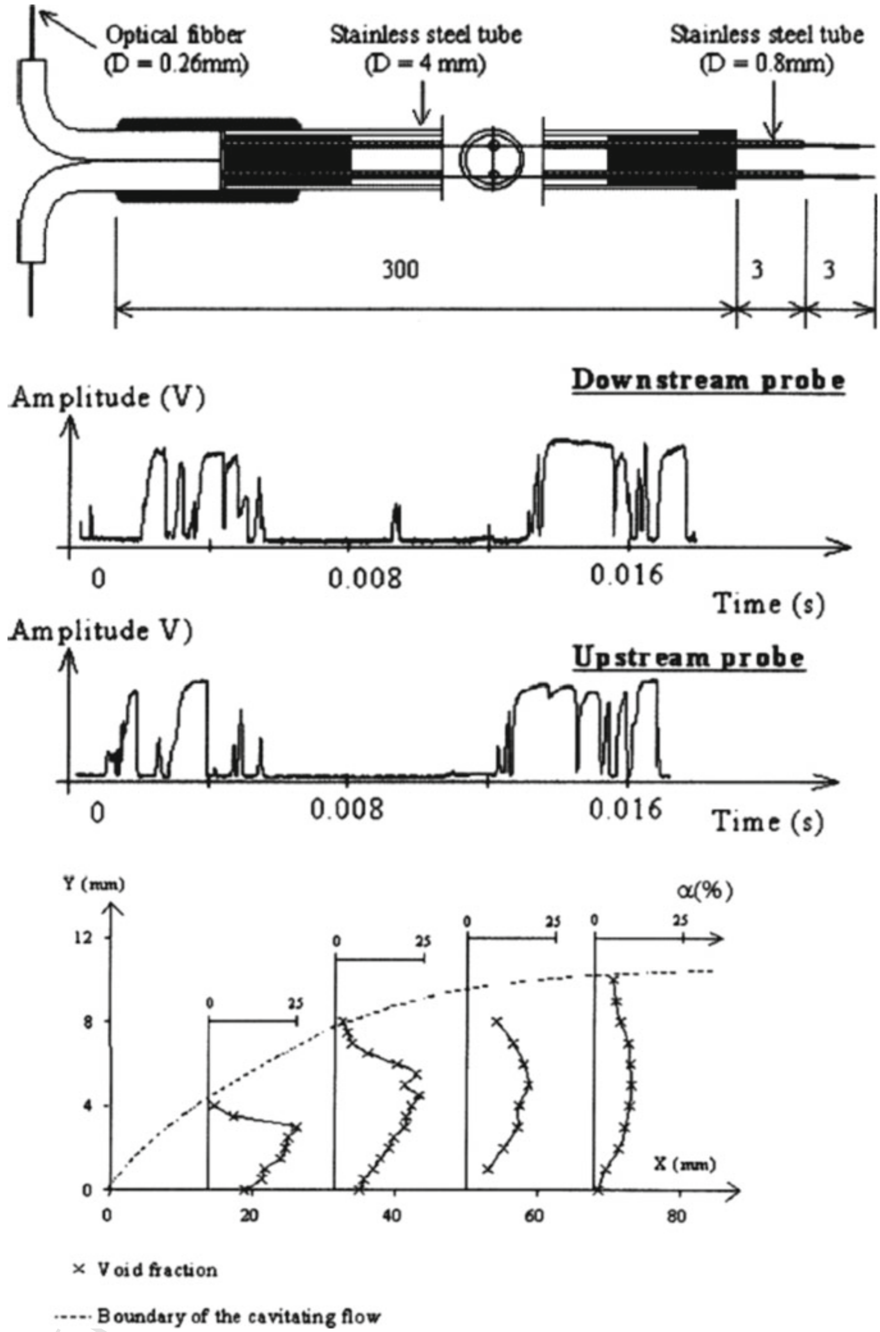

Fig. 12 The fiber optic probe used by Stutz and Reboud (2000) to measure flow within a partial cavity (**a**), example the time traces from two probes that can be used to measure volume fraction and phase speed (**b**), and a plot showing the average volume fraction within the cavity (**c**)

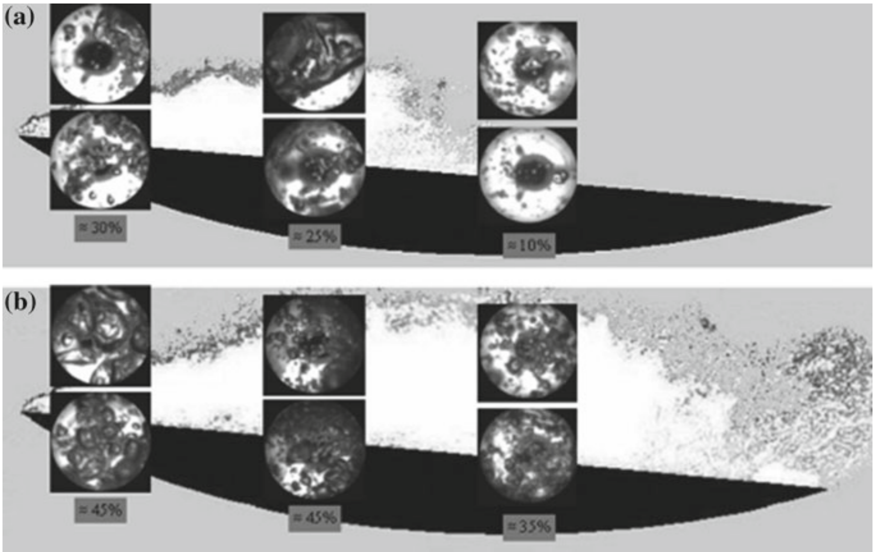

Fig. 13 Images of the bubbly flow within a partial cavity obtained by traversing an endoscope into the bubbly mixture (Coutier-Delgosha et al. 2006)

Beer–Lambert law provides a relationship between the transmitted, I, and incident, I_O, beam intensity:

$$\frac{I}{I_O} = e^{-\sum_{n=1}^{N} x_n \mu_n / \rho_n}$$

The attenuation coefficient is a function of material properties and photon energy, and is a known property for most common materials. Given this relationship, we can determine the void fraction, α, of a two-phase mixture, M, of liquid, L, and gas, G, for a monochromatic beam of photons:

$$\alpha = \ln\left(\frac{I_M}{I_L}\right) / \ln\left(\frac{I_G}{I_L}\right)$$

The transmitted beam intensities I_L, I_G, and I_M are values obtained for the pure liquid, pure gas, and mixture, respectively. For densitometry, average mixture void fraction is determined along a known linear beam path, while tomography involves the reconstruction of the two- or three-dimensional spatial distribution of attenuation through many measurements of linear path-averaged attenuation.

Stutz and Legoupil (2003) used X-ray densitometry to nonintrusively measure void fraction in a partial cavity. The setup consisted of a single row of 24 detectors that could acquire void fraction profiles along a line at a rate of 1000 samples per second. The measurements were compared with optical probes, and it was found that the maximum void fraction for the case of periodic shedding was about 25%.

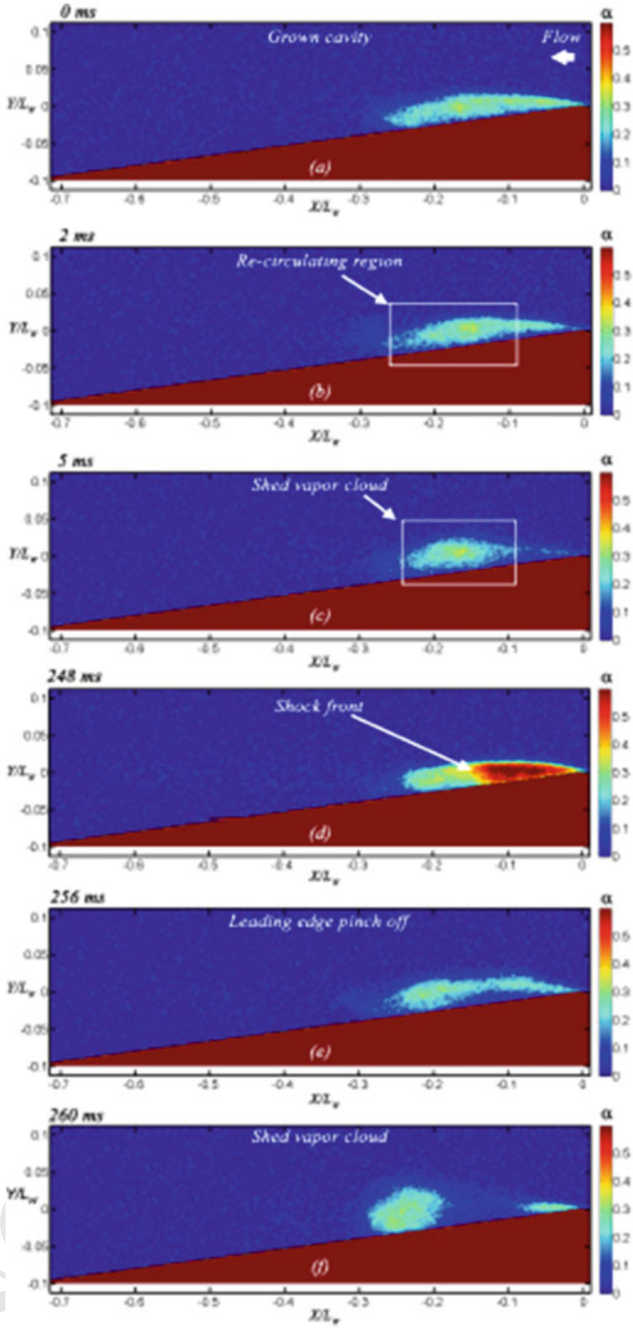

Fig. 14 A time series of X-ray densitometry-based images of a shedding partial cavity illustrating the presence of a condensation shock (Ganesh et al. 2016)

337316_1_En_2_Chapter ✓ TYPESET ☐ DISK ☐ LE ✓ CP Disp.:3/12/2016 Pages: 31 Layout: T1-Standard

Coutier-Delgosha et al. (2007) used the same diagnostic setup to measure void fraction profiles on a plano-convex foil. They reported a maximum averaged void fraction values of close to 60% with instantaneous values exceeding 85%. These systems provided the time- and phase-averaged void fraction averaged across the span of the cavity. Mäkiharju et al. (2013) recently developed an cinemagraphic X-ray densitometry system that measures two-dimensional void fraction flow fields of gas–liquid flows, and this system was used to examine the dynamic void fraction within shedding partial cavities with frame rates up to 1000 per second Ganesh et al. (2016). Figure 14 shows X-ray densitometry images of the partial cavity forming at the apex of a wedge revealing the presence of a condensation shock. While the spatial and temporal resolution of these radiation-based techniques is presently nonideal for many cavitating flows, rapid technological advances (e.g., in X-ray detectors) will make these nonintrusive techniques increasingly useful.

Acknowledgements The first author is grateful to Prof. Salvetti and Prof. d'Agostino for their invitation to the Udine summer course on cavitating flows. The authors wish to acknowledge the support of the U.S. Office of Naval Research and the U.S. Naval Sea Systems Command for their ongoing support of their research.

References

Acosta, A. J., & Parkin, B. R. (1975). Cavitation inception-a selective review. *Journal of Ship Research*, *19*(4), 193–205.
Adrian, R. J., & Westerweel, J. (2011). *Particle image velocimetry*. Cambridge University Press.
Arndt, R. E. (1981). Cavitation in fluid machinery and hydraulic structures. *Annual Review of Fluid Mechanics*, *13*(1), 273–326.
Arndt, R. E. (2002). Cavitation in vortical flows. *Annual Review of Fluid Mechanics*, *34*(1), 143–175.
Atlar, M. (2002). Final report of the specialist committee on water quality and cavitation. In *Proceedings of the 23rd ITTC*.
Avellan, F., Henry, P., & Ryhming, I. L. (1987). A new high speed cavitation tunnel for cavitation studies in hydraulic machinery. *Proceedings of international cavitation research facilities and techniques* (Vol. 57, pp. 49–60). Boston: ASME Winter Annual Meeting.
Balachandar, S., & Eaton, J. K. (2010). Turbulent dispersed multiphase flow. *Annual Review of Fluid Mechanics*, *42*, 111–133.
Benjamin, T. B., & Ellis, A. T. (1966). The collapse of cavitation bubbles and the pressures thereby produced against solid boundaries. *Philosophical Transactions of the Royal Society of London A: Mathematical, Physical and Engineering Sciences*, *260*(1110), 221–240.
Billet, M. L. (1985). *Cavitation nuclei measurements—a review*. Forum: Proceedings of ASME Cavitation and Multiphase Flow.
Boyer, C., Duquenne, A. M., & Wild, G. (2002). Measuring techniques in gas-liquid and gas-liquid-solid reactors. *Chemical Engineering Science*, *57*(16), 3185–3215.
Brandner, P. A., Lecoffre, Y., & Walker, G. J. (2007). Design considerations in the development of a modern cavitation tunnel. *Proceedings of the 16th Australasian fluid mechanics conference* (pp. 630–637).
Brennen, C. E. (1995). *Cavitation and bubble dynamics*. Cambridge University Press.
Callenaere, M., Franc, J. P., Michel, J., & Riondet, M. (2001). The cavitation instability induced by the development of a re-entrant jet. *Journal of Fluid Mechanics*, *444*, 223–256.

Cartellier, A. (1992). Simultaneous void fraction measurement, bubble velocity, and size estimate using a single optical probe in gas-liquid two-phase flows. *Review of Scientific Instruments*, *63*(11), 5442–5453.

Ceccio, S. L. (2010). Friction drag reduction of external flows with bubble and gas injection. *Annual Review of Fluid Mechanics*, *42*, 183–203.

Ceccio, S. L., & Brennen, C. E. (1991). Observations of the dynamics and acoustics of travelling bubble cavitation. *Journal of Fluid Mechanics*, *233*, 633–660.

Ceccio, S. L., & Brennen, C. E. (1992). Dynamics of attached cavities on bodies of revolution. *Journal of Fluids Engineering*, *114*(1), 93–99.

Ceccio, S. L., & George, D. L. (1996). A review of electrical impedance techniques for the measurement of multiphase flows. *Journal of Fluids Engineering*, *118*(2), 391–399.

Ceccio, S. L., Gowing, S., & Gindroz, B. (1995). A comparison of csm bubble detection methods. In Proceedings of A.S.M.E. symposium on cavitation and gas-liquid flows in fluid machinery. FED (Vol. 226, pp. 43–50).

Chahine, G. L., & Kalumuck, K. M. (2003). Development of a near real-time instrument for nuclei measurement: The abs acoustic bubble spectrometer. *Proceedings of A.S.M.E./J.S.M.E. 4th joint fluids summer engineering conference* (pp. 183–191).

Chahine, G. L., & Shen, Y. T. (1986). Bubble dynamics and cavitation inception in cavitation susceptibility meters. *Journal of Fluids Engineering*, *108*(4), 444–452.

Chambers, S. D., Bartlett, R. H., & Ceccio, S. L. (2000). Hemolytic potential of hydrodynamic cavitation. *Journal of Biomechanical Engineering*, *122*(4), 321–326.

Chang, K. A., Lim, H. J., & Su, C. B. (2003). Fiber optic reflectometer for velocity and fraction ratio measurements in multiphase flows. *Review of Scientific Instruments*, *74*(7), 3559–3565.

Chang, N., Ganesh, H., Yakushiji, R., & Ceccio, S. L. (2011). Tip vortex cavitation suppression by active mass injection. *Journal of Fluids Engineering*, *133*(11301), 1–11.

Chang, N. A., & Ceccio, S. L. (2011). The acoustic emissions of cavitation bubbles in stretched vortices. *The Journal of the Acoustical Society of America*, *130*(5), 3209–3219.

Chang, N. A., & Dowling, D. R. (2009). Ray-based acoustic localization of cavitation in a highly reverberant environment. *Journal of the Acoustical Society of America*, *125*(5), 3088–3100.

Choi, J., & Ceccio, S. L. (2007). Dynamics and noise emission of vortex cavitation bubbles. *Journal of Fluid Mechanics*, *575*, 1–26.

Coutier-Delgosha, O., Devillers, J. F., Pichon, T., Vabre, A., Woo, R., & Legoupil, S. ([illegible]). Internal structure and dynamics of sheet cavitation. *Physics of Fluids*, *18*(017103), 1–1[illegible]

Coutier-Delgosha, O., Stutz, B., Vabre, A., & Legoupil, S. (2007). Analysis of cavitating flow structure by experimental and numerical investigations. *Journal of Fluid Mechanics*, *578*, 171–222.

d'Agostino, L., & Acosta, A. J. (1991). A cavitation susceptibility meter with optical cavitation monitoring–part one: Design concepts. *Journal of Fluids Engineering*, *113*(2), 261–269.

Dular, M., Bachert, R., Stoffel, B., & Širok, B. (2005). Experimental evaluation of numerical simulation of cavitating flow around hydrofoil. *European Journal of Mechanics-B/Fluids*, *24*(4), 522–538.

Duraiswami, R., Prabhukumar, S., & Chahine, G. L. (1998). Bubble counting using an inverse acoustic scattering method. *Journal of the Acoustical Society of America*, *104*(5), 2699–2717.

Durst, F. (1982). Review–combined measurements of particle velocities, size distributions, and concentrations. *Journal of Fluids Engineering*, *104*(3), 284–296.

Elbing, B. R., Mäkiharju, S. A., Wiggins, A., Perlin, M., Dowling, D. R., & Ceccio, S. L. (2013). On the scaling of air layer drag reduction. *Journal of Fluid Mechanics*, *717*, 484–513.

Escaler, X., Egusquiza, E., Farhat, M., Avellan, F., & Coussirat, M. (2006). Detection of cavitation in hydraulic turbines. *Mechanical Systems and Signal Processing*, *20*(4), 983–1007.

Etter, R. J., Cutbirth, J. M., Ceccio, S. L., Dowling, D. R., & Perlin, M. (2005). High reynolds number experimentation in the U.S. Navy's William B. Morgan large cavitation channel. *Measurement Science and Technology*, *16*(9), 1701–1709.

Foeth, E. J., Van Doorne, C. W. H., Van Terwisga, T., & Wieneke, B. (2006). Time resolved PIV and flow visualization of 3D sheet cavitation. *Experiments in Fluids*, *40*(4), 503–513.

Ganesh, H., Mäkiharju, S. A., & Ceccio, S. L. (2016). Bubbly shock propagation as a mechanism for sheet-to-cloud transition of partial cavities. *Journal of Fluid Mechanics*.
George, D. L., Iyer, C. O., & Ceccio, S. L. (2000a). Measurement of the bubbly flow beneath partial attached cavities using electrical impedance probes. *Journal of Fluids Engineering*, *122*(1), 151–155.
George, D. L., Torczynski, J. R., Shollenberger, K. A., O'Hern, T. J., & Ceccio, S. L. (2000b). Validation of electrical-impedance tomography for measurements of material distribution in two-phase flows. *International Journal of Multiphase Flow*, *26*(4), 549–581.
Gindroz, B. (1998). Cavitation nuclei and cavitation inception of marine propellers: State of the art at the dawn of the 21st century. *J.S.M.E. International Journal Series B*, *41*(2), 464–471.
Gindroz, B., & Billet, M. L. (1998). Influence of the nuclei on the cavitation inception for different types of cavitation on ship propellers. *Journal of Fluids Engineering*, *120*(1), 171–178.
Goldstein, R. (1996). *Fluid mechanics measurements*. CRC Press.
Gopalan, S., & Katz, J. (2000). Flow structure and modeling issues in the closure region of attached cavitation. *Physics of Fluids*, *12*(4), 895–911.
Gopalan, S., Katz, J., & Knio, O. (1999). The flow structure in the near field of jets and its effect on cavitation inception. *Journal of Fluid Mechanics*, *398*, 1–43.
Gowing, S., Briançon-Marjollet, L., Frechou, D., & Godeffroy ,V. (1995). Dissolved gas and nuclei effects on tip vortex cavitation inception and cavitating core size. In *Proceedings of 5th international symposium on cavitation* (pp. 173–180).
Hassan, Y. A., Blanchat, T. K., Seeley, C. H., & Canaan, R. E. (1992). Simultaneous velocity measurements of both components of a two-phase flow using particle image velocimetry. *International Journal of Multiphase Flow*, *18*(3), 371–395.
Heindel, T. J. (2011). A review of X-ray flow visualization with applications to multiphase flows. *Journal of Fluids Engineering*, *133*(074001), 1–16.
Hewitt, G. F. (1978). *Measurement of two phase flow parameters*. Academic Press.
Iyer, C. O., & Ceccio, S. L. (2002). The influence of developed cavitation on the flow of a turbulent shear layer. *Physics of Fluids*, *14*(10), 3414–3431.
Katz, J., & Acosta, A. (1981). Observations of nuclei in cavitating flows. *Proceedings of I.U.T.A.M. symposium on mechanics and physics of bubbles in liquids* (pp. 123–132).
Katz, J., & Sheng, J. (2010). Applications of holography in fluid mechanics and particle dynamics. *Annual Review of Fluid Mechanics*, *42*, 531–555.
Katz, J., Gowing, S., O'Hern, T., & Acosta, A. (1984). A comparative study between holographic and light-scattering techniques of microbubble detection. *Proceedings of I.U.T.A.M. symposium on measuring techniques in gas-liquid two-phase flows* (pp. 41–66).
Kawanami, Y., Kato, H., Yamaguchi, H., Maeda, M., & Nakasumi, S. (2002). Inner structure of cloud cavity on a foil section. *J.S.M.E. International Journal Series B Fluids and Thermal Engineering*, *45*(3), 655–661.
Keller, A. P. (1972). The influence of the cavitation nucleus spectrum on cavitation inception, investigated with a scattered light counting method. *Journal of Fluids Engineering*, *94*(4), 917–925.
Keller, A. P. (1987). A vortex-nozzle cavitation susceptibility meter in routine application in cavitation inception measurements. In *Proceedings of euromech colloquium 222-unsteady cavitation and its effects*.
Keller, A. P. (2001). Cavitation scale effects—empirically found relations and the correlation of cavitation number and hydrodynamic coefficients. In *Proceedings of fourth international symposium on cavitation-CAV2001*.
Kjeldsen, M., Arndt, R. E. A., & Effertz, M. (2000). Spectral characteristics of sheet/cloud cavitation. *Journal of Fluids Engineering*, *122*(3), 481–487.
Kling, C. L., & Hammitt, F. G. (1972). A photographic study of spark-induced cavitation bubble collapse. *Journal of Fluids Engineering*, *94*(4), 825–832.
Koivula, T. (2000). On cavitation in fluid power. In *Proceedings of 1st FPNI-PhD symposium, Hamburg* (pp. 371–382).

Kubota, A., Kato, H., Yamaguchi, H., & Maeda, M. (1989). Unsteady structure measurement of cloud cavitation on a foil section using conditional sampling technique. *Journal of Fluids Engineering*, *111*(2), 204–210.

Kuhn de Chizelle, Y., Ceccio, S. L., & Brennen, C. E. (1995). Observations and scaling of travelling bubble cavitation. *Journal of Fluid Mechanics*, *293*, 99–126.

Kuiper, G. (1985). Reflections on cavitation inception. In *Proceedings of A.S.M.E. cavitaiton and multiphase flow forum*, FED-23.

Kumar, S. B., Dudukovic, M. P., Chaouki, J., Larachi, F., & Dudukovic, M. P. (1997). Computer assisted gamma and x-ray tomography: Applications to multiphase flow systems. *Non-invasive monitoring of multiphase flows* (pp. 47–103).

Laberteaux, K. R., & Ceccio, S. L. (2001a). Partial cavity flows. part 1. cavities forming on models without spanwise variation. *Journal of Fluid Mechanics*, *431*, 1–41.

Laberteaux, K. R., & Ceccio, S. L. (2001b). Partial cavity flows. part 2. cavities forming on test objects with spanwise variation. *Journal of Fluid Mechanics*, *431*, 43–63.

Lauterborn, W., & Bolle, H. (1975). Experimental investigations of cavitation-bubble collapse in the neighbourhood of a solid boundary. *Journal of Fluid Mechanics*, *72*(2), 391–399.

Lauterborn, W., & Hentschel, W. (1985). Cavitation bubble dynamics studied by high speed photography and holography: Part one. *Ultrasonics*, *23*(6), 260–268.

Lavigne, S. (1991). Le venturi analyseur de germes. *Journees DRET Cavitation*.

Le, Q., Franc, J. P., & Michel, J. M. (1993). Partial cavities: Pressure pulse distribution around cavity closure. *Journal of Fluids Engineering*, *115*(2), 249–254.

Le Corre, J.-M., Hervieu, E., Ishii, M., & Delhaye, J.-M. (2003). Benchmarking and improvements of measurement techniques for local-time-averaged two-phase flow parameters. *Experiments in fluids*, *35*(5), 448–458.

Lecoffre, Y., & Bonnin, J. (1979). Cavitation tests and nucleation control. In *Proceedings of A.S.M.E. international symposium on cavitation inception* (pp. 141–145).

Lecoffre, Y., Chantrel, P., & Teiller, J. (1987). Le grand tunnel hydrodynamique (GTH): France's new large cavitation tunnel for naval hydrodynamics research. In *Proceedings of A.S.M.E. international symposium on cavitation research facilities and techniques* (pp. 13–18).

Lee, I.-H., Mäkiharju, S., Ganesh, H., & Ceccio, S. L. (2016). Scaling of gas diffusion into limited partial cavities. *Journal of Fluids Engineering*.

Leger, A. T., & Ceccio, S. L. (1998). Examination of the flow near the leading edge of attached cavitation. part 1. detachment of two-dimensional and axisymmetric cavities. *Journal of Fluid Mechanics*, *376*, 61–90.

Leger, A. T., Bernal, L. P., & Ceccio, S. L. (1998). Examination of the flow near the leading edge of attached cavitation. part 2. incipient breakdown of two-dimensional and axisymmetric cavities. *Journal of Fluid Mechanics*, *376*, 91–113.

Li, C. Y., & Ceccio, S. L. (1996). Interaction of single travelling bubbles with the boundary layer and attached cavitation. *Journal of Fluid Mechanics*, *322*, 329–353.

Lindken, R., & Merzkirch, W. (2002). A novel piv technique for measurements in multiphase flows and its application to two-phase bubbly flows. *Experiments in Fluids*, *33*(6), 814–825.

Lucas, G. P., & Mishra, R. (2005). Measurement of bubble velocity components in a swirling gas-liquid pipe flow using a local four-sensor conductance probe. *Measurement Science and Technology*, *16*(3), 749–758.

Mäkiharju, S. A., Gabillet, C., Paik, B.-G., Chang, N. A., Perlin, M., & Ceccio, S. L. (2013). Time-resolved two-dimensional x-ray densitometry of a two-phase flow downstream of a ventilated cavity. *Experiments in Fluids*, *54*(7), 1–21.

McNulty, P. J., & Pearsall, I. S. (1982). Cavitation inception in pumps. *Journal of Fluids Engineering*, *104*(1), 99–104.

Mørch, K. A. (2007). Reflections on cavitation nuclei in water. *Physics of Fluids*, *19*(072104), 1–7.

Obreschkow, D., Kobel, P., Dorsaz, N., De Bosset, A., Nicollier, C., & Farhat, M. (2006). Cavitation bubble dynamics inside liquid drops in microgravity. *Physical Review Letters*, *97*(094502), 1–4.

O'Hern, T. J., Katz, J., & Acosta, A. J. (1985). *Holographic measurements of cavitation nuclei in the sea*. In Proceedings of A: S.M.E. cavitation and multiphase flow forum.

Ohl, C. D., Philipp, A., & Lauterborn, W. (1995). Cavitation bubble collapse studied at 20 million frames per second. *Annalen der Physik*, *507*(1), 26–34.

Ohl, C. D., Lindau, O., & Lauterborn, W. (1998). Luminescence from spherically and aspherically collapsing laser induced bubbles. *Physical Review Letters*, *80*(2), 393–396.

Oldenziel, D. M. (1982). A new instrument in cavitation research: the cavitation susceptibility meter. *Journal of Fluids Engineering*, *104*(2), 136–141.

Oweis, G. F., Choi, J., & Ceccio, S. L. (2004). Dynamics and noise emission of laser induced cavitation bubbles in a vortical flow field. *Journal of the Acoustical Society of America*, *115*(3), 1049–1058.

Pham, T. M., Larrarte, F., & Fruman, D. H. (1999). Investigation of unsteady sheet cavitation and cloud cavitation mechanisms. *Journal of Fluids Engineering*, *121*(2), 289–296.

Rae, W. H., & Pope, A. (1984). *Low-speed wind tunnel testing*, 2nd edition. Wiley.

Ran, B., & Katz, J. (1994). Pressure fluctuations and their effect on cavitation inception within water jets. *Journal of Fluid Mechanics*, *262*, 223–263.

Rood, E. P. (1991). Review–mechanisms of cavitation inception. *Journal of Fluids Engineering*, *113*(2), 163–175.

Rooze, J., Rebrov, E. V., Schouten, J. C., & Keurentjes, J. T. (2013). Dissolved gas and ultrasonic cavitation-a review. *Ultrasonics Sonochemistry*, *20*(1), 1–11.

Roth, H., Gavaises, M., & Arcoumanis, C. (2002). *Cavitation initiation, its development and link with flow turbulence in diesel injector nozzles*. S.A.E. Technical Paper, (2002-01-0214).

Sato, R., Mori, T., Yakushiji, R., Naganuma, K., Nishimura, M., Nakagawa, K., & Sasajima, T. (2003). Conceptual design of the flow noise simulator. In *Proceedings of joint A.S.M.E./J.S.M.E. 4th joint fluids summer engineering conference* (pp. 129–133).

Schiebe, F. R. (1972). Measurement of the cavitation susceptibility of water using standard bodies. *St. Anthony Falls Laboratory Project Report 118*, University of Minnesota.

Shen, Y. T., & Dimotakis, P. E. (1989). Viscous and nuclei effects on hydrodynamic loadings and cavitation of a naca 66 (mod) foil section. *Journal of Fluids Engineering*, *111*(3), 306–316.

Simoni, R. D., Hill, R. L., & Vaughan, M. (2002). The measurement of blood gases and the manometric techniques developed by donald dexter van slyke. *Journal of Biological Chemistry*, *277*(27), e16.

Straka, W. A., Meyer, R. S., Fontaine, A. A., & Welz, J. P. (2010). Cavitation inception in quiescent and co-flow nozzle jets. *Journal of Hydrodynamics, Series B*, *22*(5), 813–819.

Stutz, B. (2003). Influence of roughness on the two-phase flow structure of sheet cavitation. *Journal of Fluids Engineering*, *125*(4), 652–659.

Stutz, B., & Legoupil, S. (2003). X-ray measurements within unsteady cavitation. *Experiments in Fluids*, *35*(2), 130–138.

Stutz, B., & Reboud, J. L. (2000). Measurements within unsteady cavitation. *Experiments in Fluids*, *29*(6), 522–545.

Tanger, H., & Weitendorf, E. A. (1992). Applicability tests for the phase doppler anemometer for cavitation nuclei measurements. *Journal of Fluids Engineering*, *114*(3), 443–449.

Thoroddsen, S. T., Etoh, T. G., & Takehara, K. (2008). High-speed imaging of drops and bubbles. *Annual Review of Fluid Mechanics*, *40*, 257–285.

Tropea, C., Yarin, A. L., & Foss, J. F. (Eds.). (2007). *Springer handbook of experimental fluid mechanics*. Springer Science and Business Media.

Van der Kooij, J., & De Bruijn, A. (1984). Acoustic measurements in the NSMB depressurized towing tank. *International Shipbuilding Progress*, *31*(353), 13–25.

Vogel, A., & Lauterborn, W. (1988). Time-resolved particle image velocimetry used in the investigation of cavitation bubble dynamics. *Applied Optics*, *27*(9), 1869–1876.

Wetzel, J. M., & Arndt, R. E. A. (1994a). Hydrodynamic design considerations for hydroacoustic facilities: Part I- flow quality. *Journal of Fluids Engineering*, *116*(2), 324–331.

Wetzel, J. M., & Arndt, R. E. A. (1994b). Hydrodynamic design considerations for hydroacoustic facilities: Part II- pump design factors. *Journal of Fluids Engineering*, *116*(2), 332–337.

Wosnik, M., Schauer, T. J., & Arndt, R. E. (2003). Experimental study of a ventilated supercavitating vehicle. In *Proceedings of fifth international symposium on cavitation* (pp. 1–4).

Wu, Q., & Ishii, M. (1999). Sensitivity study on double-sensor conductivity probe for the measurement of interfacial area concentration in bubbly flow. *International Journal of Multiphase Flow*, *25*(1), 155–173.

Yu, P. W., & Ceccio, S. L. (1997). Diffusion induced bubble populations downstream of a partial cavity. *Journal of Fluids Engineering*, *119*(4), 782–787.

Author Queries

Chapter 2

Query Refs.	Details Required	Author's response
AQ1	Please provide high-resolution source file for Fig. 14.	
AQ2	Please check and confirm if the inserted citation of Fig. 13 is correct. If not, please suggest an alternate citation. Please note that figures should be cited sequentially in the text.	

MARKED PROOF

Please correct and return this set

Please use the proof correction marks shown below for all alterations and corrections. If you wish to return your proof by fax you should ensure that all amendments are written clearly in dark ink and are made well within the page margins.

Instruction to printer	*Textual mark*	*Marginal mark*
Leave unchanged	• • • under matter to remain	Ⓥ
Insert in text the matter indicated in the margin	⋏	New matter followed by ⋏ or ⋏ⓧ2
Delete	/ through single character, rule or underline or ⊢⊣ through all characters to be deleted	∂ or ∂ⓧ2
Substitute character or substitute part of one or more word(s)	/ through letter or ⊢⊣ through characters	new character / or new characters /
Change to italics	— under matter to be changed	⌴
Change to capitals	≡ under matter to be changed	≡
Change to small capitals	= under matter to be changed	=
Change to bold type	~ under matter to be changed	~
Change to bold italic	≂ under matter to be changed	≂
Change to lower case	Encircle matter to be changed	≢
Change italic to upright type	(As above)	⍭
Change bold to non-bold type	(As above)	⍭
Insert 'superior' character	/ through character or ⋏ where required	Y or X under character e.g. Y or X
Insert 'inferior' character	(As above)	⋏ over character e.g. ⋏
Insert full stop	(As above)	⊙
Insert comma	(As above)	,
Insert single quotation marks	(As above)	Y or X and/or Y or X
Insert double quotation marks	(As above)	Y or X and/or Y or X
Insert hyphen	(As above)	⊢⊣
Start new paragraph	⌐	⌐
No new paragraph	↩	↩
Transpose	⊔⊓	⊔⊓
Close up	linking ◯ characters	◯
Insert or substitute space between characters or words	/ through character or ⋏ where required	Y
Reduce space between characters or words	| between characters or words affected	T